

Patterning and growth of carbon nanotubes on a highly structured 3D substrate surface

This article has been downloaded from IOPscience. Please scroll down to see the full text article.

2009 J. Micromech. Microeng. 19 105009

(<http://iopscience.iop.org/0960-1317/19/10/105009>)

View [the table of contents for this issue](#), or go to the [journal homepage](#) for more

Download details:

IP Address: 140.114.59.160

The article was downloaded on 21/08/2012 at 05:46

Please note that [terms and conditions apply](#).

Patterning and growth of carbon nanotubes on a highly structured 3D substrate surface

Wang-Shen Su¹, Chia-Min Lin², Ting-Hsien Chen² and Weileun Fang^{1,2,3,4}

¹ National Nano Device Laboratories, Hsinchu, Taiwan

² Institute of NanoEngineering and MicroSystems, National Tsing Hua University, Hsinchu, Taiwan

³ Department of Power Mechanical Engineering, National Tsing Hua University, Hsinchu, Taiwan

E-mail: fang@pme.nthu.edu.tw

Received 12 July 2009, in final form 10 August 2009

Published 16 September 2009

Online at stacks.iop.org/JMM/19/105009

Abstract

This study demonstrates the patterning and growth of carbon nanotubes (CNTs) on a highly structured three-dimensional (3D) substrate surface and even underneath the suspended microstructure surface. Three key processes—plasma surface treatment, self-assembled monolayer (SAM) coating and contact displacement electroless (CDE) plating—are employed and integrated to implement the present concept. In application, the CNTs have been conformally grown and patterned on the highly structured 3D substrate surface containing 100 μm deep anisotropic etched cavities with 54.7° as well as 90° sidewalls. The integration of these 3D patterns of CNTs with suspended MEMS cantilevers has also been demonstrated. Moreover, the ‘positive’ and ‘negative’ pattern transformations of CNTs on the highly structured substrate surface and even underneath the suspended MEMS structure surface are successfully achieved. In addition, the 3D patterns of CNTs have also been successfully transferred onto flexible PDMS substrates.

(Some figures in this article are in colour only in the electronic version)

1. Introduction

Carbon nanotubes (CNTs) show unique chemical, mechanical and electronic properties, and can be fabricated into micro-devices; for instance, implantation of structured CNT arrays into chip-scale microelectronics has been previously demonstrated and devices exhibit a large working deflection upon application of an ac field [1]. In addition, the CNTs have been used as a device component of sensors [2, 3], actuators [4, 5], electromechanical oscillators [6] and even a CNT radio [7]. Besides, a CNT cantilever has been used for nanotweezers [8], a scanning probe microscope tip [9] and switches [10, 11]. In short, the integration of CNTs and micro-electromechanical systems (MEMS) can find various applications. The implementation of CNTs on a substrate and the integration of CNTs with the existing micro-fabrication processes are critical concerns for these applications.

Presently, the integration of CNT arrays onto a silicon substrate mainly relies on assembly techniques. Batch fabrication processes, such as lithography, offset printing and thermal growth, to implement CNTs on a substrate are usually constrained on a planar surface [12–15]. In general, the substrate containing MEMS devices has a complicated surface profile containing, for instance, cavities, mesas, suspensions, etc. This limits the potential of using CNTs for MEMS applications. The integration of suspended carbon nanotubes with MEMS devices has been successfully demonstrated [16]. In addition, various process technologies, such as modified spin coating [17], electrodeposition (ED) [18–24] and the spray coating technique [23–26], have been reported to implement MEMS devices on a highly structured 3D substrate surface. However, controlled fabrication of CNT structures on highly structured surfaces has so far remained a great challenge.

⁴ Author to whom any correspondence should be addressed.

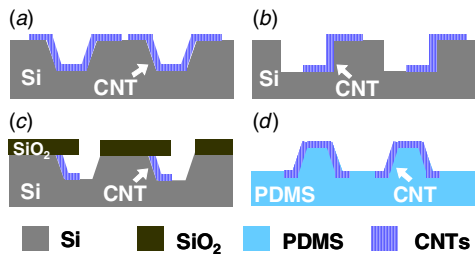


Figure 1. The concept of 3D CNTs on Si/polymer substrate with a highly structured surface.

This work extends the planar-based CNT structures to 3D profiles; meanwhile, the integration of 3D-patterned CNTs into suspended MEMS devices is also achieved. This study exploits three key processes—plasma treatment [27–29], self-assembled coating of octadecyltrichlorosilane (OTS) monolayer and contact displacement electrolless (CDE) plating [30, 31]—to prevent the limitation of complicated surface topology imposed by photolithography and film deposition processes. Thus, as shown in figure 1, the present processes can implement (1) conformal formation of 3D CNT patterns on a highly structured Si surface, as shown in figures 1(a) and (b), (2) further integration of these 3D patterns of CNTs with suspended MEMS devices, as shown in figure 1(c), and (3) transfer of the 3D patterns of CNTs onto flexible polymer substrates, as shown in figure 1(d).

2. Fabrication processes

Figure 2 illustrates the process steps established in this study. As shown in figures 2(a1)–(a4), the silicon substrate

containing deep cavities and suspended thin film structures were first prepared using bulk micromachining processes. After that the substrate then experienced a 30 min surface treatment using uncollimated O₂ plasma at 250 °C, 500 mTorr and 300 W in a plasma-enhanced chemical vapor deposition (PECVD) chamber. Thus, the Si–O bond was formed on the substrate surface, as indicated in figures 2(a1) and (a2). On the other hand, the silicon substrate could also experience the treatment of uncollimated H₂ plasma to form Si–H bonds on the substrate surface, as shown in figures 2(a3) and (a4). In addition, the substrate surface covered with Si–O bonds was further immersed into anhydrous toluene solution containing 1 vol.% OTS for 1 h under a N₂ atmosphere. Thus, the formation of OTS self-assembled monolayer (OTS-SAM) on the substrate surface with Si–O bonds was achieved, as shown in figures 2(a1) and (a2). This approach enabled full and conformal coverage of OTS-SAM on substrates with the highly structured surfaces (e.g., a surface with deep cavities, or the surface underneath the suspended microstructures). The OTS and Si–H layers on the highly structured surface were patterned by the collimated O₂ plasma, and the shape of these layers could be defined either by a shadow mask (as shown in figures 2(b1) and (b3)) or by the suspended thin film structure (as depicted in figures 2(b2) and (b4)). The commercially made shadow mask was fabricated using laser micromachining on a silicon wafer. The minimum line width of the shadow mask was 50 μm for a 250 μm thick wafer, and became 100 μm for a 500 μm thick wafer. In addition, the minimum line width can be further reduced to 20 μm using the deep reactive ion etching (DRIE) process. As a result, the OTS bombarded by the O₂ plasma was removed so as to selectively

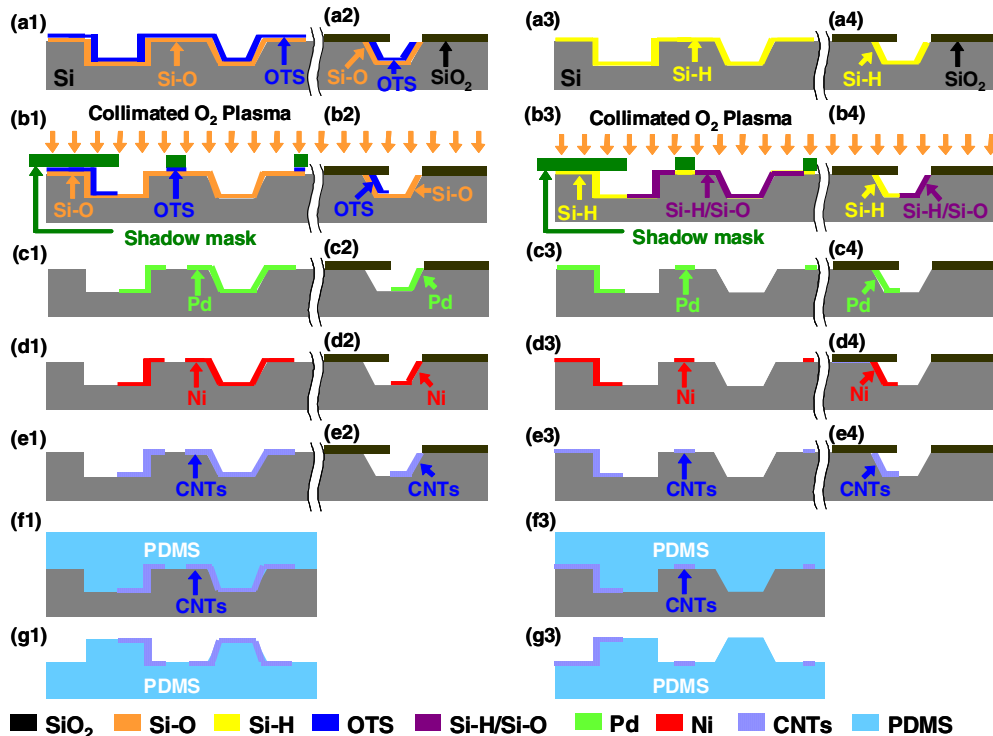
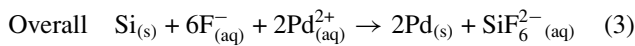
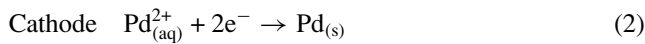
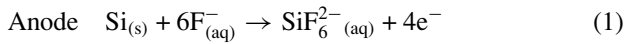


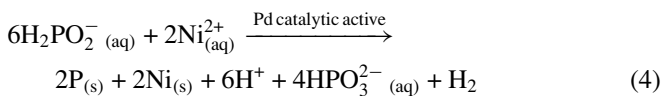
Figure 2. The fabrication process flow to grow and pattern CNTs on a highly structured 3D substrate surface.

expose the Si–O bond on the substrate surface, as shown in figures 2(b1) and (b2). On the other hand, some of the Si–H bonds bombarded by the collimated O₂ plasma were replaced by Si–O bonds, as shown in figures 2(b3) and (b4). This collimated O₂ plasma patterning process was operated in a high-density plasma reactive ion etching (HDP-RIE) system. The variation of pattern dimension (e.g., line width) from the top surface of the substrate to the bottom surface of the cavity was tuned by varying O₂ plasma conditions such as the inductively coupled plasma (ICP) radio frequency (RF) power and dc bias.

The CDE plating process [30, 31] was then employed to selectively deposit a thin nickel (Ni) catalyst layer on the highly structured substrate surface. In brief, the CDE plating consisted of the selective displacement of the palladium (Pd) activation layer shown in figure 2(c), and the electroless plating of the Ni layer shown in figure 2(d). The contact displacement of Pd ions from silicon was first carried out by the electrochemical redox between Si⁰ and Pd²⁺ ions in BOE (buffered oxide etchant containing F[−]):



The chemical reaction depicted in equation (3) occurred only after the removal of the Si–O bond indicated in figure 2(b) by BOE. Since the Si–O bond covered by OTS was not etched by BOE, the underneath Si was not replaced by the Pd activation layer. Thus, the Pd activation layer was selectively plated on the highly structured substrate surface without OTS (figures 2(c1) and (c2)). The etching rate of the Si–H bond in BOE was faster than that of the Si–H/Si–O bond, and further caused the selectivity of Pd activation. Thus, the Pd activation layer in figures 2(c3) and (c4) was only plated on the highly structured substrate surface with Si–H bonds. After that the electroless plating of the Ni layer within a NiSO₄–NaH₂PO₂ bath [32, 33] was performed. The Ni film was autocatalytically deposited in the highly structured substrate surface with the Pd activation layer:



In other words, the Ni film in figures 2(d1) and (d2) was selectively plated on the highly structured substrate surface with OTS, while the Ni film in figures 2(d3) and (d4) was only plated on the highly structured substrate surface with Si–H bonds.

The Ni film in figure 2(d) was employed to act as the catalyst layer for the growth of CNTs. The CNTs were then grown on the highly structured substrate surface by acetylene pyrolysis at 800 °C in a gas mixture of Ar, NH₃ and C₂H₂, as illustrated in figure 2(e). Moreover, the molding process was employed to transfer patterned CNTs onto the flexible PDMS substrate with the highly structured surface, as shown in figures 2(f) and (g). The PDMS polymer (SYLGARD 184 silicone elastomer, base:curing agent = 10:1)

was poured onto the mold-substrate (figures 2(f1) and (f3)), and the air trapped inside the cavity was fully removed by a vacuum pump. The molded PDMS attached to the mold substrate was cured at 100 °C for 1 h. Finally, the flexible PDMS substrate with patterned CNTs on the highly structured surface was demolded from the mold-substrate, as illustrated in figures 2(g1) and (g3).

As illustrated in figure 2(b), the present O₂ plasma lithography technology enables pattern transformation on the highly structured substrate surface using the shadow mask (figures 2(b1) and (b3)) as well as suspended thin film structures (figures 2(b2) and (b4)). Thus, the suspended thin film structure has no alignment issue during pattern transformation. Moreover, as indicated in figures 2(b1)–(e1), the CNTs will grow in the area exposed to the O₂ plasma for the OTS approach. On the other hand, as indicated in figures 2(b3)–(e3), the CNTs will not grow in the area exposed to the O₂ plasma for the Si–H approach. In other words, the OTS and Si–H can be respectively employed to act as ‘positive’ and ‘negative’ pattern transformation layers during the O₂ plasma lithography.

3. Results and discussions

As demonstrated in figure 3, the CNTs patterned on the highly structured substrate surface were fabricated using the processes shown in figures 2(a1)–(e1). The SEM (scanning electron microscope) micrographs in figure 3(a) show the patterned CNT arrays (100 μm line width) distributed on a 3D silicon surface with 100 μm deep anisotropically etched cavities. The 54.7° inclination of cavity sidewalls was formed by the (111) crystal planes of the silicon substrate, and the sidewalls were patterned using the TMAH (tetramethyl ammonium hydroxide) anisotropic chemical etching process. The enlarged SEM micrograph in figure 3(b) shows that the patterned CNTs are well distributed on the highly structured substrate surface with various crystal planes (the (100) top surface, the 54.7° (111) sidewalls and the (100) bottom surface). The SEM micrograph in figure 3(c) further demonstrates the growth of CNTs on a substrate surface with near 90° Si sidewalls (50 μm deep). The silicon sidewalls were patterned using anisotropic DRIE. The enlarged SEM micrograph in figure 3(d) clearly shows the CNTs at the edge of near 90° sidewall. It is very challenging to deposit the Ni catalyst and then to grow the CNTs on the highly structured substrate surface with 90° sidewalls using existing approaches [12–15, 17–26].

The SEM micrographs in figure 4 show the oval shape patterns defined on the highly structured silicon surface using the same shadow mask. Figure 4(a) shows a silicon substrate containing a 100 μm deep bulk micromachined cavity. This highly structured silicon substrate has only oval shape CNT patterns grown and distributed on its surface. The enlarged micrograph in figure 4(b) further demonstrates the oval shape pattern formed by the CNTs. These oval shape CNT patterns were defined by means of the ‘positive’ pattern transformation approach using the shadow mask. On the other hand, the SEM micrograph in figure 4(c) also shows a silicon

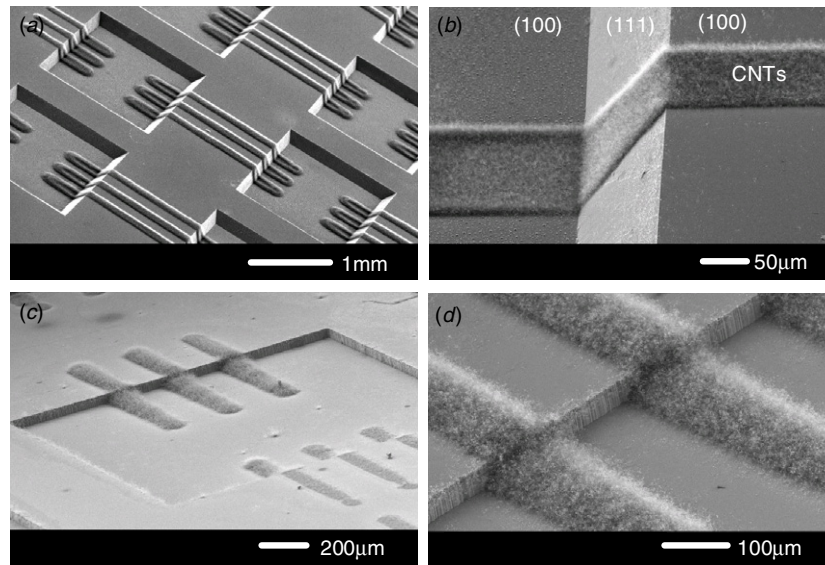


Figure 3. The SEM micrographs of 3D CNT patterns distributed on a highly structured silicon surface: (a) and (b) bulk etched cavity with 54.7° (111) crystal-plane sidewalls, and (c) and (d) bulk etched cavity with 90° sidewalls.

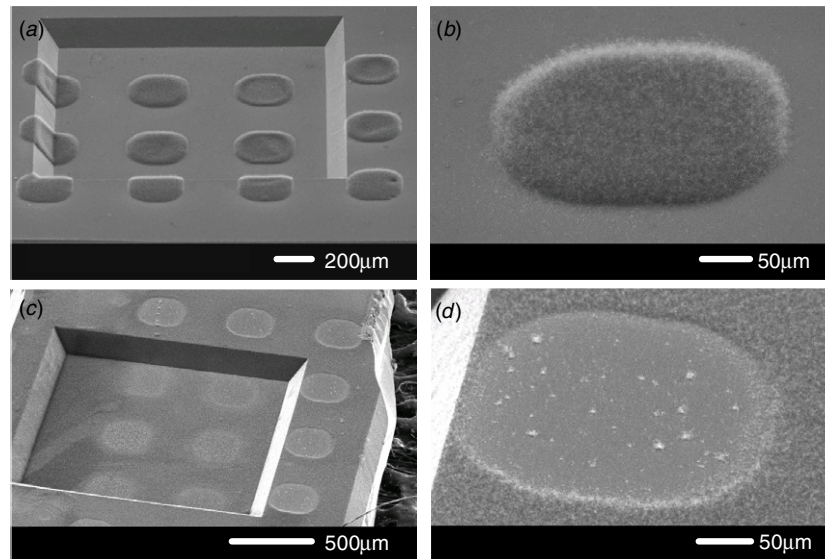


Figure 4. The SEM micrographs of 3D CNT patterns distributed on silicon surfaces with 54.7° sidewall cavity: (a) and (b) fabricated by the 'positive' pattern transformation approach, and (c) and (d) fabricated by the 'negative' pattern transformation method.

substrate containing a $100\ \mu\text{m}$ deep bulk micromachined cavity. However, the CNTs are grown and distributed all over the highly structured silicon substrate surface except the oval shape patterns. The enlarged micrograph in figure 4(d) further demonstrates the oval shape pattern with no CNTs. These oval shape patterns were defined by means of the 'negative' pattern transformation approach using the same shadow mask as that for figure 4(a).

The SEM micrographs in figure 5 demonstrate the fabrication results using the suspended thin film structures as the mask for pattern transformation. The SEM micrograph in figure 5(a) shows the suspended SiO_2 micro-cantilever array fabricated using the TMAH anisotropic chemical etching. The enlarged micrograph in figure 5(b) clearly demonstrates the selective growth of CNTs on the $150\ \mu\text{m}$

deep bulk micromachined cavity where the SiO_2 cantilever array suspended. Since the 'positive' pattern transformation was employed in this case, the CNTs were grown on the whole cavity except the region shadowed by the cantilever. Moreover, the micrograph in figure 5(c) shows the selective growth of CNTs using the 'negative' pattern transformation of the suspended SiO_2 micro-cantilever array. The enlarged micrograph in figure 5(d) also demonstrates the selective growth of CNTs on the $150\ \mu\text{m}$ deep cavity. Since the 'negative' pattern transformation was employed in this case, the CNTs were only grown on the region shadowed by the cantilever. Note that existing photolithography cannot pattern the Ni catalyst at regions underneath the suspended microstructures [12–15, 17–26]. In short, this study successfully employs the shadow mask as well as the thin film

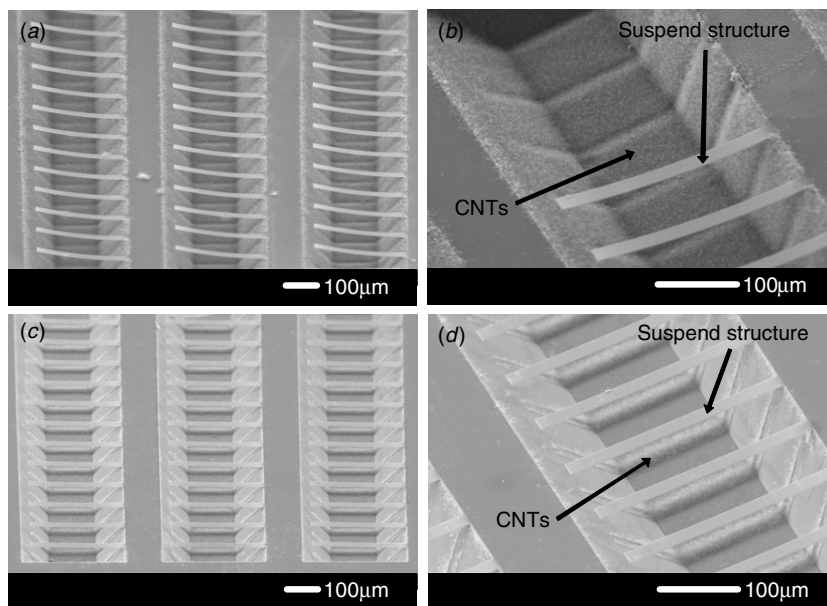


Figure 5. The SEM micrographs of 3D CNT patterns distributed on silicon surfaces with suspended SiO₂ micro-cantilevers: (a) and (b) fabricated by the ‘positive’ pattern transformation method, so that the region shadowed by the suspended cantilever has no CNTs, and (c) and (d) fabricated by the ‘negative’ pattern transformation method, so that only the region shadowed by the suspended cantilever has CNTs.

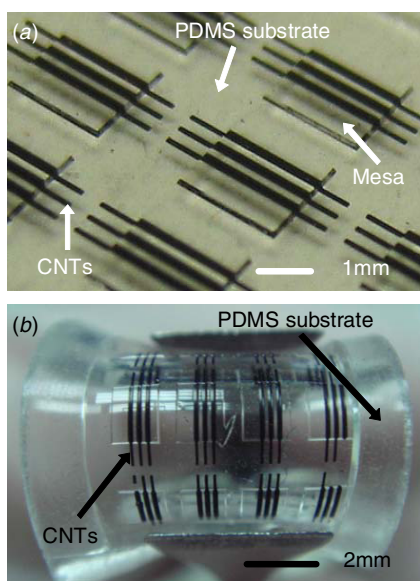


Figure 6. The optical microscope image of typical fabrication results containing 3D CNT patterns on flexible polymer substrate using the molding process.

suspended microstructures to demonstrate the ‘positive’ and the ‘negative’ pattern transformation on a highly structured substrate surface.

The optical image in figure 6(a) exhibits the successful transfer of CNT structures (black region) onto a flexible PDMS substrate (transparent region) via the molding process shown in figures 2(f) and (g). After the molding process, about 93% CNTs were transferred onto the flexible PDMS substrate, and the other 7% of CNTs remained adhered to the mold-substrate. As shown in figure 6(b), the particular bending of CNTs built on PDMS substrate demonstrates the structural flexibility.

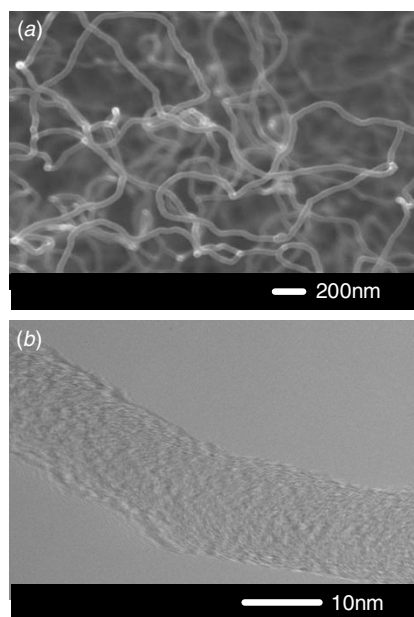


Figure 7. (a) The FE-SEM micrograph for the nanostructure of CNTs, and (b) the TEM image showing the bamboo-like structured CNTs grown on Ni catalysts.

The CNTs grown in the present processes were characterized using field emission scanning electron microscopy (FE-SEM), transmission electron microscopy (TEM) and Raman spectroscopy. The current–voltage (*I*–*V*) curve of the CNTs was also characterized. Figure 7(a) shows the FE-SEM image of CNTs grown by the Ni catalyst. The CNTs exhibit a tubular nanostructure and form a net of nanotubular chains. The TEM image in figure 7(b) shows that the CNTs are multi-walled with bamboo-like structure. The average diameter of CNTs is about 20–50 nm. As shown in figure 8, the Raman spectra

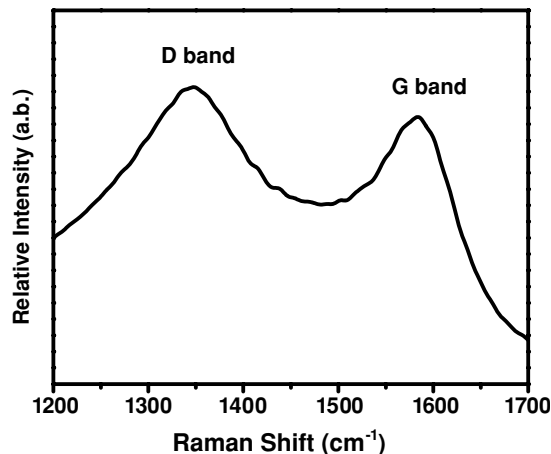


Figure 8. The Raman spectra of the CNTs grown using the present process.

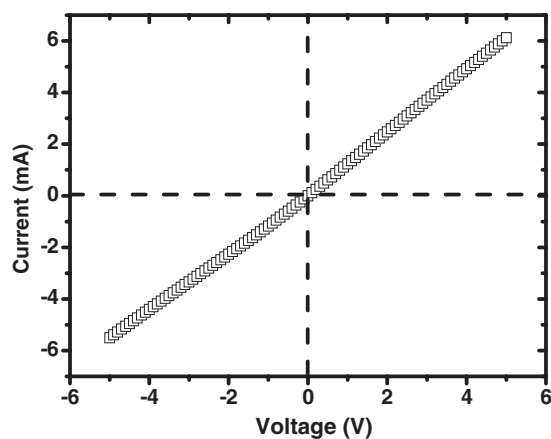


Figure 9. The I - V curves of the CNTs grown using the present process.

for CNTs reveal two Raman bands at $\sim 1335\text{ cm}^{-1}$ (D-band) and $\sim 1580\text{ cm}^{-1}$ (G-band). The D-band to G-band intensity ratio (I_D/I_G) for the present CNTs is 1.6. The electrical resistance of the CNTs was estimated from the measured I - V curve shown in figure 9. The linear curve indicates a good ohmic characteristic, and the corresponding resistance is $0.85\text{ k}\Omega$.

4. Conclusions

In summary, this study accomplishes 3D lithography on a highly structured substrate surface using SAM coating and plasma treatment approaches. O_2 and H_2 plasmas are employed to treat the surface of the Si substrate so as to provide selectivity for the following CDE plating. Moreover, the selective Ni-catalyst layer deposition as well as the growth of CNTs on the 3D surface and even underneath the suspended microstructures is realized using the CDE plating and the acetylene pyrolysis method. As a result, the 'positive' and 'negative' pattern transformations of CNTs on the highly structured substrate surface are successfully

achieved. In application, the CNTs have been conformally grown and patterned on a highly structured 3D substrate surface containing $100\text{ }\mu\text{m}$ deep anisotropic etched cavities with 54.7° as well as 90° sidewalls. The integration of these 3D patterns of CNTs with suspended MEMS devices has also been demonstrated. In addition, the 3D patterns of CNTs have been successfully transferred onto flexible PDMS substrates. The capabilities of growing 3D CNT patterns on a complicated substrate surface and even underneath the suspended microstructures offer design flexibility for the integration of CNTs and MEMS. Since both CNTs and PDMS polymer are biocompatible, the CNTs on flexible PDMS offer the possibility for bioapplications.

Acknowledgments

This project was (partially) supported by the NSC of Taiwan under grant of NSC96-2628-E-007-008-MY3. The authors would also like to thank the Nano Science and Technology Center of National Tsing Hua University, Nano Facility Center of National Chiao Tung University, and National Nano Device Lab for providing the fabrication facilities. The authors would like to thank Dr Ming-Pei Lu for the measurement of the electronic properties of CNTs.

References

- [1] Li J, Papadopoulos C, Xu J M and Moskovits M 1999 Highly ordered carbon nanotube arrays for electronics applications *Appl. Phys. Lett.* **75** 367–69
- [2] Kong J, Franklin N R, Zhou C, Chapline M G, Peng S, Cho K and Dai H 2000 Nanotube molecular wires as chemical sensors *Science* **287** 622–25
- [3] Stampfer C, Helbling T, Oberfell D, Schöberle B, Tripp M K, Jungen A, Roth S, Bright V M and Hierold C 2006 Fabrication of single walled carbon nanotube based pressure sensors *Nano Lett.* **6** 233–7
- [4] Fennimore A M, Yuzvinsky T D, Han W Q, Fuhrer M S, Cumings J and Zettl A 2003 Rotational actuators based on carbon nanotubes *Nature* **424** 408–10
- [5] Hayamizu Y, Yamada T, Mizuno K, Davis R C, Futaba D N, Yumura M and Hata K 2008 Integrated three-dimensional microelectromechanical devices from processable carbon nanotube wafers *Nat. Nanotechnol.* **3** 289–94
- [6] Sazonova V, Yaish Y, Üstünel H, Roundy D, Arias T A and McEuen P L 2004 A tunable carbon nanotube electromechanical oscillator *Nature* **431** 284–7
- [7] Jensen K, Weldon J, Garcia H and Zettl A 2007 Nanotube radio *Nano Lett.* **7** 3508–11
- [8] Kim P and Lieber C M 1999 Nanotube nanotweezers *Science* **286** 2148–50
- [9] Dai H, Hafner J H, Rinzler A G, Colbert D T and Smalley R E 1996 Nanotubes as nanoprobe in scanning probe microscopy *Nature* **384** 147–50
- [10] Deshpande V V, Chiu H Y, Postma H W Ch, Mikó C, Forró L and Bockrath M 2006 Carbon nanotube linear bearing nanoswitches *Nano Lett.* **6** 1092–5
- [11] Jang J E, Cha S N, Choi Y J, Kang D J, Butler T P, Hasko D G, Jung J E, Kim J M and Amaratunga G A J 2008 Nanoscale memory cell based on a nanoelectromechanical switched capacitor *Nat. Nanotechnol.* **3** 26–30
- [12] Fan S, Chapline M G, Franklin N R, Tomblor T W, Cassell A M and Dai H 1999 Self oriented regular arrays of

- carbon nanotubes and their field emission properties *Science* **283** 512–14
- [13] Wei B Q, Vajtai R, Jung Y, Ward J, Zhang Y, Ramanath G and Ajayan P M 2002 Organized assembly of carbon nanotubes *Nature* **416** 495–6
- [14] Gu G, Philipp G, Wu X, Burghard M, Bittner A M and Roth S 2001 Growth of single walled carbon nanotubes from microcontact printed catalyst patterns on thin Si₃N₄ membranes *Adv. Funct. Mater.* **11** 295–8
- [15] Sohn J I, Lee S, Song Y, Choi S, Cho K and Nam K 2001 Patterned selective growth of carbon nanotubes and large field emission from vertically well aligned carbon nanotube field emitter arrays *Appl. Phys. Lett.* **78** 901–3
- [16] Karp G A, Ya'akovovitz A, David-Pur M, Ioffe Z, Cheshnovsky O, Krylov S and Hanein Y 2009 Integration of suspended carbon nanotubes into micro-fabricated devices *J. Micromech. Microeng.* **19** 085021
- [17] Kutshoukov V G, Shikida M, Mollinger J R and Bossche A 2004 Through wafer interconnect technology for silicon *J. Micromech. Microeng.* **14** 1029–36
- [18] Larsson M P and Syms R R A 2004 Self aligning MEMS in-line separable electrical connector *J. Microelectromech. Syst.* **13** 365–76
- [19] Pham N P, Boellaard E, Wien W, Van Den Brekel L D M, Burghartz J N and Sarro P M 2004 Metal patterning on high topography surface for 3D RF devices fabrication *Sensors Actuators A* **115** 557–62
- [20] Richard Å, Rangsten P, Strandman C and Bäcklund Y 1999 Decreasing the optical path length in an optoelectronic module using silicon micromachining *J. Micromech. Microeng.* **9** 127–9
- [21] Loechel B 2000 Thick-layer resists for surface micromachining *J. Micromech. Microeng.* **10** 108–15
- [22] O'Brien J, Hughes P J, Brunet M, O'Neill B, Alderman J, Lane B, O'Riordan A and O'Driscoll C 2001 Advanced photoresist technologies for microsystems *J. Micromech. Microeng.* **11** 353–8
- [23] Pham N P, Boellaard E, Burghartz J N and Sarro P M 2004 Photoresist coating methods for the integration of novel 3-D RF microstructures *J. Microelectromech. Syst.* **13** 491–9
- [24] Pham N P, Tezcan D S, Ruythooren W, De Moor P, Majeed B, Baert K and Swinnen B 2008 Photoresist coating and patterning for through-silicon via technology *J. Micromech. Microeng.* **18** 125008
- [25] Singh V K, Sasaki M, Hane K, Watanabe Y, Takamatsu H, Kawakita M and Hayashi H 2005 Deposition of thin and uniform photoresist on three-dimensional structures using fast flow in spray coating *J. Micromech. Microeng.* **15** 2339–45
- [26] Pham N P, Burghartz J N and Sarro P M 2005 Spray coating of photoresist for pattern transfer on high topography surfaces *J. Micromech. Microeng.* **15** 691–7
- [27] Su W S, Lee S T, Lin C Y, Yip M C, Tsai M S and Fang W 2006 Tuning the shape and curvature of micromachined cantilever using multiple plasma treatments technology *Sensors Actuators A* **130–131** 553–9
- [28] Su W S, Lee S T, Lin C Y, Yip M C, Tsai M S and Fang W 2006 Control the shape of buckling micromachined beam using plasma chemistry bonding technology *Japan. J. Appl. Phys.* **45** 8479–83
- [29] Su W S, Huang H Y and Fang W 2008 Modification of the mechanical properties of SiO₂ thin film using plasma treatments for micro-electro-mechanical systems applications *Japan. J. Appl. Phys.* **47** 5242–7
- [30] Lee Y P, Tsai M S, Hu T C, Dai B T and Feng M S 2001 Selective copper metallization by electrochemical contact displacement with amorphous silicon film *Electrochem. Solid State Lett.* **4** C47–9
- [31] Su W S, Tsai M S and Fang W 2007 A three dimensional microfabrication technology on highly structured surfaces *Electrochem. Solid State Lett.* **10** H16–19
- [32] Salvago G and Cavallotti P L 1972 Characteristics of the chemical reduction of nickel alloys with hypophosphite *Plating* **59** 665–71
- [33] Van Den Meerakker J E A M 1981 On the mechanism of electroless plating: II. One mechanism for different reductants *J. Appl. Electrochem.* **11** 395–400